Journal of Photochemistry and Photobiology A: Chemistry 217 (2011) 395–401

Contents lists available at ScienceDirect

Journal of Photochemistry and Photobiology A: Chemistry

journal homepage: www.elsevier.com/locate/jphotochem

Spectroscopic studies on pH- and thermally induced conformational changes of Bovine Serum Albumin adsorbed onto gold nanoparticles

Monica Iosin*, Valentin Canpean, Simion Astilean*

Nanobiophotonics Center, Institute of Interdisciplinary Research in Bio-NanoSciences and Faculty of Physics, Babes-Bolyai University, M. Kogalniceanu 1, 400084 Cluj-Napoca, Romania

ARTICLE INFO

Article history:
Received 20 August 2010
Received in revised form 27 October 2010
Accepted 16 November 2010
Available online 23 November 2010

Keywords:
Nano–bio interface
Gold nanoparticles
Bovin Serum Albumin
Tryptophan
Fluorescence
SERS

ABSTRACT

In this work we used gold nanoparticles (GNPs) as probes to evaluate the pH- and temperature-induced conformational changes of Bovine Serum Albumin (BSA) adsorbed on their surface. UV–vis and fluorescence spectroscopy were employed to monitor the adsorption and binding modes of BSA on GNPs. The results suggest that GNPs quenched the fluorescence emission of tryptophan residues of BSA mainly through a static mechanism, the binding constant (K_b) being sensitive to the pH values. The Stern–Volmer quenching constant (K_{SV}) and the corresponding thermodynamic parameters (ΔH, ΔS and ΔG) were also determined. In addition, the results concerning the thermally induced conformation changes of BSA, before and after interfacing with GNPs, demonstrate the dependence of the protein conformational transition temperature on pH. Moreover, the linking between BSA and GNPs was monitored by surface-enhanced Raman scattering (SERS), assessing the influence of pH on this specific nano–bio interface.

1. Introduction

A new trend in nanoscience concerns the development of novel nanomaterials, exhibiting outstanding physical, chemical and biological properties, and the exploitation of their behavior in biological applications. The development of suitable nano–bio-conjugates for relevant and specific biomedical applications and the achievement of a profound understanding of the synergism between these biological systems and nanoparticles are important issues that must be addressed. The exploitation of surface plasmons sustained by metallic nanostructures offers the possibility of developing novel devices that can be used for bio-chemical mapping at nanometer scale [1]. In this sense, due to their chemical stability and unique optical properties, dominated by the excitation of localized surface plasmon resonance (LSPR), gold nanoparticles (GNPs) are attractive nanomaterials for surface enhanced Raman scattering (SERS) [2], metal-enhanced fluorescence (MEF) [3,4] and localized surface plasmon resonance (LSPR) sensors [5]. Additionally, due to their biocompatibility and surface chemistry which allows their facile conjugation with different biomolecules, GNPs are ideal probes for the investigation of biological processes, localized photo-thermal therapy of tumors, and localized and controlled drug delivery [6,7]. However, it is well known that the interaction of proteins with GNPs is highly sensitive to the particles surface chemistry and the conformational state of the protein [8]. In this context, a major challenge remains to investigate the conformational behavior of proteins in a protein–nanoparticles conjugated system, including denaturation of their tertiary and secondary structures, which is susceptible to occur due to protein adsorption [9]. Brewer et al. demonstrated the interaction between citrate-coated GNPs and Bovine Serum Albumin (BSA) proteins [10] and more recently De Paoli Lacerda et al. reported the specific interaction between GNPs and human plasma proteins [11]. Moreover, Guo et al. demonstrated the possibility of using GNPs as probes to investigate the conformational change of poly-L-lysine in the range of pH from 6.5 to 11.0 [12]. In addition, we demonstrated, using spectroscopic techniques, the direct interaction between BSA and GNPs, assessing the influence of the GNPs surface on the binding of albumin, providing information concerning the possible protein conformation changes induced after bioconjugation [13]. However, thermodynamic parameters, such as temperature and pH, can also trigger the disruption of protein conformation which could lead to cancer, diabetes and cardiovascular diseases [14] and consequently can have a major influence on the nano–bio interfaces.

Therefore, to gain a better insight on the nano–bio interaction, it is clearly of great interest to extend our previous studies by

* Corresponding authors at: Babes-Bolyai University, Institute of Interdisciplinary Research in Bio-NanoSciences, Nanobiophotonics Center, Treboniu Laurian 42, 400271 Cluj-Napoca, Romania. Tel.: +40 264 454554/119; fax: +40 264 591906.
E-mail addresses: monica.iosin@phys.ubbcluj.ro (M. Iosin), simion.astilean@phys.ubbcluj.ro (S. Astilean).

1010-6030/$ – see front matter © 2010 Elsevier B.V. All rights reserved.
doi:10.1016/j.jphotochem.2010.11.012

integrating the effects of pH and temperature on the nano–bio conjugates. To address this issue we investigate the interface between GNPs and BSA, as a function of pH and temperature, by employing three different spectroscopic techniques: LSPR, fluorescence and SERS. BSA is a globular protein with the approximate ellipsoidal shape of 4 nm × 4 nm × 14 nm [15], widely used for bio-nanotechnology applications [16]. The native structure of BSA is characterized by a single polypeptide chain composed of 583 amino-acid residues, its tertiary structure comprising three homologous domains (I, II and III), each one formed by six helices, which are stabilized by an internal network of 17 disulfide bonds [17]. However, the conformation of BSA is highly dependent on pH and temperature, each conformational state being characterized by its own shape and dimension. In this context, Raman and fluorescence spectroscopy, due to their high sensitivity, were employed in complementary manner to provide valuable information concerning protein conformational changes, induced by the interactions with GNPs, pH and temperature. Fluorescence spectroscopy, an ideal and powerful technique to evaluate protein conformational changes, was used to monitor the intrinsic emission characteristics of tryptophan (Trp) residues in albumin in order to demonstrate the local interaction between albumin and GNPs, and subsequently, to investigate the pH and thermally induced conformational changes of BSA. We found that pH has a major impact on the nano–bio interfaces, influencing the binding constant, number of binding sites and quenching constant. Moreover, the detection of conformational changes of the protein as well as the specific interaction with GNPs with respect to pH was confirmed by SERS measurements. In view of future biological applications, we also investigated the heat-induced changes in the tertiary structure of both free and bioconjugated BSA, assessing different pH specific critical temperatures at which conformational changes of BSA are susceptible to occur.

2. Materials and methods

2.1. Materials

Tetrachloroauric acid ($HAuCl_4{\cdot}4H_2O$, 99.99%), sodium citrate ($C_6H_5Na_3O_7$), aminopropyltriethoxysilane (APS) and Bovine Serum Albumin (BSA, MW 66 kDa) were purchased from Aldrich and used as received. Reagent-grade NaOH and HCl were used to adjust the pH values. Ultra-pure water with a conductivity of 18.2 MΩ was used throughout the experiments.

2.2. Gold nanospheres synthesis and conjugation with BSA

Spherical GNPs with a diameter of about 18 ± 2 nm (determined from TEM image) were synthesized according to the Turkevich method, which uses the reduction of chloroauric acid ($HAuCl_4$) with sodium citrate [18]. The as-prepared nanoparticles exhibit a plasmonic resonance peak at 520 nm.

The albumin solutions were prepared freshly at room temperature by dissolving solid BSA in ultrapure water at pH 6 to a concentration of 1 mg/mL, which corresponds to the native form of BSA. The solution was adjusted to pH 2 and pH 5 by the addition of small volumes of 0.1 M HCl and to pH 9, respectively, by the addition of 0.1 M NaOH solution. The albumin solutions were stirred for 30 min to ensure complete protein dissolution. The BSA–GNPs bioconjugates were prepared by mixing 100 μL of BSA solution, at different pH values, with 500 μL of GNPs solution. The as-prepared BSA–GNPs solution was used for the UV–vis measurements. For the fluorescence measurements various BSA–GNPs solutions were prepared by mixing the BSA and GNPs solutions in different molar ratios between 1:0 and 1:6. The concentrations of GNPs were ranged from 0.55×10^{-9} M to 2.75×10^{-9} M. All pH measurements were made with a 315 I pH meter.

2.3. Substrate preparation for SERS analysis

For SERS measurements, the preparation of GNPs substrate comprises a few steps: (i) the glass slides were treated in Piranha solution (3:1 H_2SO_4:H_2O_2) for 24 h in order to remove the organic groups; (ii) the cleaned glass slides were functionalized in APS MeOH for 1 h; (iii) the as-prepared substrates were rinsed several times with MeOH and ultrapure water; (iv) the silanized substrates were immersed in colloidal GNPs solution for 120 min; (v) the substrates coated with GNPs were immersed for 2 h into the BSA protein solution at different pH.

2.4. Characterization of the BSA–GNPs bioconjugates

The optical absorbance spectra of the prepared solutions were recorded at room temperature using a Jasco V-670 UV–vis-NIR spectrophotometer with a slit width of 2 nm. The morphology and size distribution of as-formed GNPs were analyzed by transmission electron microscopy (TEM) using a JEOL JEM 1010 microscope. For BSA–nanoparticles conjugates imaging, the negative staining technique was employed using uranyl acetate dihydrate as the contrast agent. The samples for TEM were prepared by placing a drop of gold colloidal solutions onto carbon-coated copper grids and dried at room temperature. The fluorescence spectra were recorded using a Jasco LP-6500 spectrofluorimeter coupled with a Jasco ADP-303T temperature controller (−10 to 110 °C). The intrinsic fluorescence of BSA was obtained at 337 nm by exciting the fluorescence of Trp residues at 280 nm using bandwidths of 3 nm and quartz cells with 1.0 cm path length. The SERS measurements were conducted using a Confocal Raman microscope (CRM 200 Witec) equipped with a 100× microscope objective. The spectra were recorded using a 632.8 nm He–Ne laser with a power of 1.5 mW. The typical exposure time for each SERS measurement was 30 s. The SERS spectra were collected from different points on the sample in order to ensure the reproducibility of the measurements.

3. Results and discussion

3.1. Monitoring the formation of BSA–GNPs bioconjugates at different pH

pH is one of the most important external stimuli that affects the conformation of the BSA protein in solution, also influencing the charge of the protein functional groups and moreover, can cause the attraction or repulsion of GNPs in solution. As such, we decided to monitor the effect of the pH on the optical response of BSA, both pure and absorbed on the surface of GNPs. We must point out that the surface of the as-prepared GNPs is negatively charged due to citrate coverage which prevents their aggregation. However, the net charge of BSA molecule is highly sensitive to the pH of the solution, being positive for pH < pI, neutral for pH = pI and negative for pH > pI, where pI represents the isoelectric point [19]. In our case, the isoelectric point of BSA is 4.7 [20]. In agreement with these observations, Fig. 1 shows the UV–vis absorption spectra of BSA solution in the absence (spectra a–c) and presence of GNPs (spectra d–f) at pH 2, 6 and 9, respectively, together with the reference spectrum (g) of the as-prepared GNPs in solution. The BSA in solution exhibits a specific absorption band in UV at about 278 nm due to the electronic transition of aromatic amino acids, slightly shifting as a function of pH. Compared to free GNPs in solution, the spectral position of the LSPR band of bioconjugated GNPs exhibited a pH sensitive red-shift, from 520 nm to 527 nm,

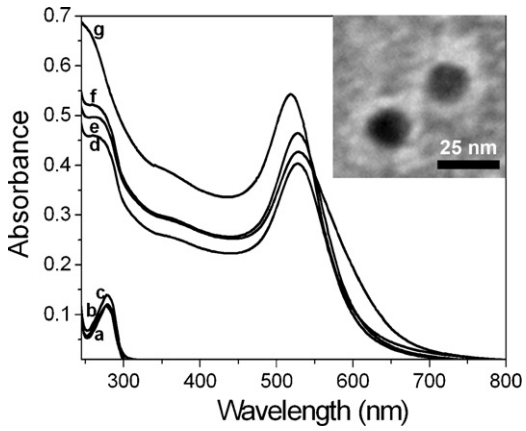

Fig. 1. Absorption spectra of BSA solution in the absence (spectra a–c) and presence of GNPs (spectra d–f) at pH 2, 6 and 9, respectively; spectrum g represents the absorption spectrum of the as-prepared GNPs in solution. The inset shows a representative TEM image of BSA–GNPs bioconjugate at pH 6.

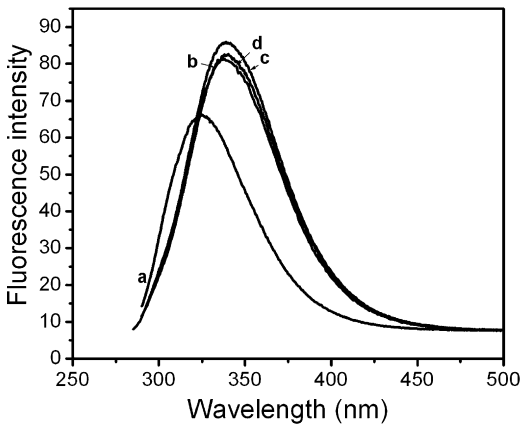

Fig. 2. Fluorescence spectra of BSA at pH 2 (spectrum a), pH 5 (spectrum b), pH 6 (spectrum c) and pH 9 (spectrum d).

523 nm and 521 nm for pH 2, pH 6 and pH 9, respectively. The LSPR spectral shifts transduce the modification of the refractive index that occurred in the local environment of the nanoparticles as a result of the formation of the bioconjugates. We infer the presence of BSA at the surface of GNPs from the TEM images (see inset in Fig. 1), which clearly reveal a white layer contour of 3.5 nm surrounding the nanoparticles, referred in the literature as "protein corona" [21]. Additionally, the measured spectral modifications were accompanied by a visual change of the solution's color, from red, corresponding to isolate GNPs, to violet, corresponding to bioconjugates. These spectral changes inform about the formation of BSA–GNPs bioconjugates which modify the electromagnetic coupling of GNPs and their optical response. At pH 2 the positive charge of BSA molecules interacts with the negatively charged GNPs, leading to a larger LSPR red shift and a concomitant broadening of the plasmonic band of GNPs. On the contrary, at high pH there is an electrostatic repulsive interaction between the negatively charged GNPs and BSA, keeping most of the GNPs isolated and stable. In addition, the interaction between BSA and GNPs was also assessed by the observed changes in the shape of the recorded absorption spectrum of BSA before and after bioconjugation (see Fig. 1). Nonetheless these results are not conclusive for obtaining relevant information concerning the conformational behavior of the albumin, due to the significant overlapping with the absorption of Au^{3+} ions and auric species in solution [22]. However, more specific information concerning the pH-induced conformational changes of BSA, as well as the degree of exposure of the Trp residues in albumin to solvent can be obtained using fluorescence spectroscopy.

In fact, the fluorescence properties of BSA are due to the existence of Trp residues in two different positions, one located on the surface of the protein in domain I (Trp-134), more exposed to a hydrophilic environment, and the other in the hydrophobic pocket in domain II (Trp-213) [23]. As we can seen in Fig. 2, the pure BSA solution at pH 6 (spectrum c) exhibits an intrinsic emission band centered at 337 nm, while at pH 2 (spectrum a), pH 5 (spectrum b) and pH 9 (spectrum d) the emission band was shifted at 324 nm, 336 nm and 339 nm, respectively, indicating different possible conformation states of albumin as a consequence of pH changes. Actually the shift of the emission maximum provides valuable information about the polarity changes around the fluorophore molecule [24], the blue shift indicating that Trp residues in albumin were placed in a more hydrophobic environment due to its tertiary structural change, whereas the red shift indicating that Trp residues were more exposed to solvent. Thus, at neutral pH, BSA presents a normal/native form ('N-form'), whereas at pH 2 and pH 9 BSA presents a fully expanded ('E-form') and basic ('B-form') form, respectively. In the 'E-form', the fluorescence emission of BSA is blue shifted compared to the 'N-form', due to the increased inter-domain separation and rearrangement of the Trp in a more hydrophobic environment of the protein matrix [25].

In order to obtain local information concerning the Trp emission behavior in albumin at different pH, in the presence of GNPs, a fixed concentration of BSA was titrated with different amounts of GNPs solution. The results presented in Fig. 3 demonstrate the drastic quenching of the fluorescence emission of the Trp residues in albumin at pH 2 with increasing concentrations of GNPs (from 0.55×10^{-11} M to 2.75×10^{-11} M). From the recorded fluorescence spectra, the quenching constant (K_{SV}) can be calculated using the Stern–Volmer equation [26]

$$\frac{F_0}{F} = 1 + K_q \tau_0 [\text{GNPs}] = 1 + K_{SV}[\text{GNPs}] \quad (1)$$

where F_0 and F are the relative fluorescence intensity of Trp residues in absence and presence of GNPs, K_q is the bimolecular quenching rate constant, $\tau_0 = 5 \times 10^{-9}$ s is the average lifetime of the BSA in the absence of GNPs, [GNPs] is the concentration of the quencher and K_{SV} is the Stern–Volmer quenching constant, which

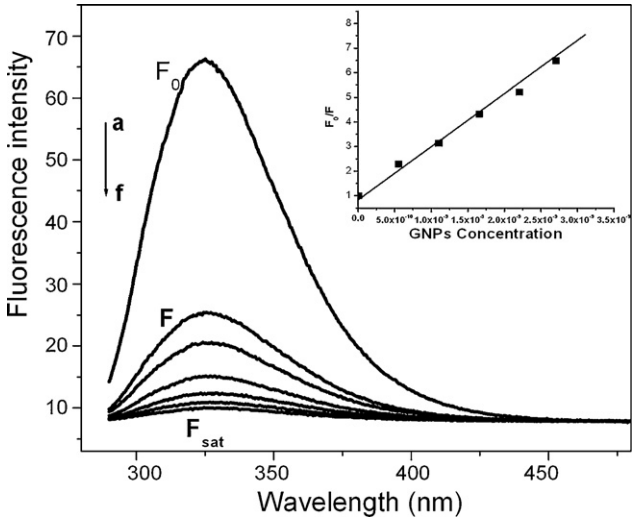

Fig. 3. The fluorescence spectra of tryptophan residues in BSA (pH 2) at different concentrations of GNPs: (a) 0, (b) 0.55×10^{-11} M, (c) 1.1×10^{-11} M, (d) 1.65×10^{-11} M, (e) 2.2×10^{-11} M and (f) 2.75×10^{-11} M. Inset shows the Stern–Volmer plot of BSA fluorescence quenching induced by GNPs at pH 2.

indicates the sensitivity of the fluorophore to a quencher. For pH 2, the Stern–Volmer curve of F_0/F versus concentration of GNPs was plotted in the inset in Fig. 3. From the linear fit of the data, we found that $K_{SV} = 1.11 \times 10^9\ M^{-1}$. Similarly, we calculated the Stern–Volmer quenching constants for pH 6 and 9 (data not shown here), yielding $K_{SV} = 1.7 \times 10^9\ M^{-1}$ for pH 6 and $K_{SV} = 1.6 \times 10^9\ M^{-1}$ for pH 9. Thus, from Eq. (1) the bimolecular quenching rate constant K_q was calculated to be $K_q = 0.22 \times 10^{18}\ M^{-1}\ s^{-1}$ for the BSA–GNPs bioconjugates at pH 2, $K_q = 0.34 \times 10^{18}\ M^{-1}\ s^{-1}$ at pH 6 and $K_q = 0.32 \times 10^{18}\ M^{-1}\ s^{-1}$ at pH 9, respectively. The calculated K_q is greater compared with the value obtained for biological macromolecules due to the collision mechanism ($2.0 \times 10^{10}\ M^{-1}\ s^{-1}$), implying that in our case the quenching is not initiated by dynamic collision but by the formation of a nonfluorescent complex resulted from static quenching mechanism [27].

The equilibrium binding constant (K_b) and the number of binding sites (n) between GNPs and BSA can be also determined from the above results, as we previously described [13]. Thus, the number of binding sites n were found to be 1.77 at pH 2, 1.97 at pH 6 and 1.76 at pH 9, whereas the binding constant K_b, which indicates the equilibrium between adsorbing and desorbing species, were calculated to be $2.6 \times 10^9\ M^{-1}$ at pH 2, $1.81 \times 10^9\ M^{-1}$ at pH 6 and $2.03 \times 10^9\ M^{-1}$ at pH 9, higher values corresponding to stronger attraction. Moreover, in order to mimic the real biological environment we specifically studied the formation of bioconjugates at pH 5 which is common in many cellular organelles. We calculated the Stern–Volmer quenching and bimolecular quenching rate constant, yielding $K_{SV} = 1.74 \times 10^9\ M^{-1}$ and $K_q = 0.348 \times 10^{18}\ M^{-1}\ s^{-1}$. The number of binding sites and the equilibrium binding constant in this case were $n = 1.85$ and $K_b = 2.82 \times 10^9\ M^{-1}$, revealing that the maximum adsorption of albumin molecules on the surface of GNPs occurs close to the pI of BSA.

3.2. Monitoring the thermal denaturation of BSA at different pH

The thermal denaturation of the proteins is an intricate process and therefore its elucidation is vital for understanding the protein stability. In fact, by increasing the temperature, the native form of the protein becomes more flexible, and as a consequence, free –SH groups or hydrophobic regions become available to new intermolecular interactions. However, the information concerning the thermal denaturation of proteins in the presence of GNPs is limited in the literature, and therefore, the second purpose of this study was to investigate the structural changes that accompany the thermal denaturation of BSA, both before and after adsorption onto the surface of GNPs, by analyzing the fluorescence emission of Trp residues in albumin. In this sense, we monitored the changes in fluorescence emission of Trp residues in albumin between 22 °C and 85 °C, a range of temperature variations which are expected to greatly influence the tertiary structure of albumin.

As we mentioned before, the pure BSA aqueous solution at room temperature exhibits a strong intrinsic fluorescence emission band centered at 337 nm, which is highly sensitive to the microenvironment [28]. As such, by increasing the temperature, the fluorescence spectrum of Trp exhibited a significant blue shift of its emission maximum from 337 nm to 330 nm. The graphical representation presented in the inset of Fig. 4 (denaturation curve) reveals a nonlinear relationship between the measured blue shift and temperature. Thus, the denaturation curve of pure BSA suggests the existence of two transition temperatures, at 43 °C and 65 °C, at which a change in the Trp environment occurs as a consequence of temperature increase leading to changes of the protein conformational structure. Interestingly, the plateau of the denaturation curve indicates that albumin maintains its native state up to about 42–43 °C and the first transition temperature occurs near the maximum temperature of fever in pathological conditions (i.e.

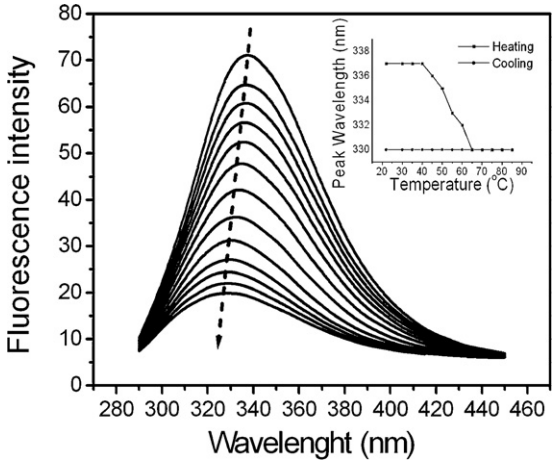

Fig. 4. Temperature dependence of the fluorescence emission spectra of Tryptophan residues in BSA at pH 6. The inset shows the temperature-induced variation of fluorescence peak position of tryptophan, both during heating and cooling.

42 °C). Between 43 °C and 65 °C a blue shift of the maximum fluorescence of albumin was observed, this drop-off of the denaturation curve of pure BSA, suggesting a transition from its compact/native state to a more open state. Rezaei-Tavirani et al. also observed a similar behavior for albumin protein using different methods [29]. The full protein denaturation ends after 65 °C where we recorded the second plateau of the denaturation curve. Additionally, in good agreement with our results, Lin and Koenig reported the same transition temperatures for BSA using Raman spectroscopy, concluding that up to 42 °C the BSA protein remains in the native state, between 50 °C and 60 °C the α-helix unfolding occurs, while at 70 °C the gel formation or intermolecular association takes place, suggesting the presence of β-conformation [30]. It is worthwhile to mention that this behavior of the denaturation curve was accompanied by a linear decrease of the intensity of the Trp emission by increasing the temperature. Thus, increasing the temperature from 22 °C to 85 °C lead to a 72% decrease of the emission intensity, due to the fully exposure of Trp residues to the solvent, which is in good agreement with the principle of micelle sensitization [31]. In addition, we investigated the reversibility of the thermal denaturation of BSA by monitoring the emission spectra of Trp during the cooling process, the results yielding an irreversible behavior of the denaturation curve of BSA (see inset Fig. 4).

Further we proceed to investigate the combined effects of temperature and pH on the behavior of BSA, before and after bioconjugation with GNPs. For this purpose we compared the thermal denaturation curve of the protein solution between 22 °C and 85 °C for four different pH values: 2 (Fig. 5, spectra ▲), 5 (Fig. 5, spectra ■), 6 (Fig. 5, spectra ●) and 9 (Fig. 5, spectra ⋆). Firstly, we observe a high dependence of the protein conformational transition temperatures on pH. Compared to pH 6, the alkaline medium has a much more drastic effect on the protein demonstrated by the lower temperature of the first transition point, which occurred at 32 °C. On the contrary, the acidic medium is less harmful to the protein, the BSA denaturation curve exhibiting in this case the first transition temperature at 46 °C. The bioconjugation with GNPs has a pH-sensitive effect on the denaturation curve of the BSA. As shown in Fig. 5, spectrum ●, at pH 6 the presence of GNPs induces a red shift of BSA emission as discussed before, yielding a first transition temperature at 47 °C. This temperature difference implies that the presence of GNPs modifies the thermal behavior of BSA fluorescence, improving thus the thermal stability of the protein. However, the thermal denaturation of the bioconjugated BSA at pH 2 and 9, exhibits similar behaviors with that of BSA before bioconjugation, at the same pH values.

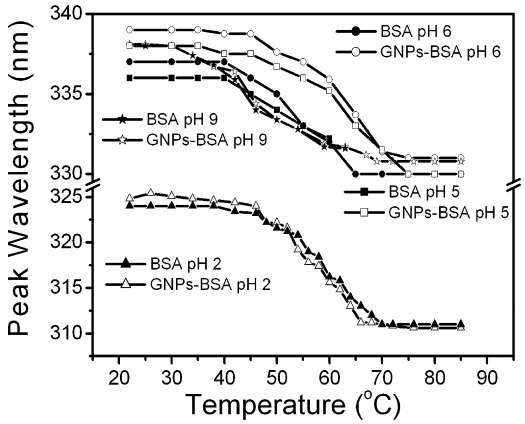

Fig. 5. Temperature-induced variation of the fluorescence emission peak position of BSA solution compared with BSA–GNPs conjugates at different pH; λ_{exc} = 280 nm.

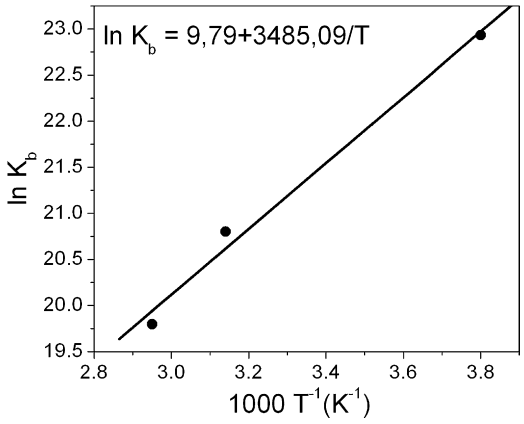

Fig. 7. Van't Hoff plot of BSA–GNPs bioconjugates at pH 6 calculated for three different temperatures.

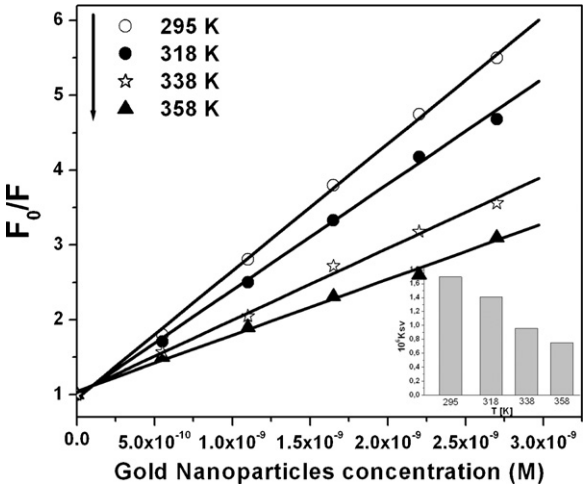

Fig. 6. Stern–Volmer plots for the quenching at pH 6 of BSA by GNPs at the four different temperatures. The inset shows the dependence of the Stern–Volmer K_{SV} quenching constant on the temperature.

In order to investigate the temperature effect on fluorescence quenching of BSA by GNPs we calculated the K_{SV} quenching constant at different temperatures. Fig. 6 presents the Stern–Volmer plots for the quenching of the Trp residues in albumin at pH 6 by the GNPs at four different temperatures (295, 318, 338, 358 K), demonstrating that the K_{SV} quenching constant is inversely correlated with temperature. The corresponding values of K_{SV} at different temperatures are presented in Table 1. This inverse proportionality between the quenching constant and temperature also confirms, as demonstrated previously, that the quenching mechanism of the BSA–GNPs binding reaction is initiated by the formation of a non-fluorescent complex between BSA molecules and GNPs quenchers [26].

3.3. Determination of the thermodynamic parameters and binding mode between BSA and GNPs

The potential interaction forces between GNPs and biological macromolecules, in general, may include hydrogen bonds, hydrophobic forces, electrostatic forces, and van der Waals' interactions, and therefore, it is important to investigate the binding mode of BSA to GNPs. In order to elucidate this interaction we proceed to a thermodynamic analysis of the GNPs-induced quenching of the fluorescence emission of BSA at three different temperatures. The standard enthalpy change (ΔH) and standard entropy change (ΔS) for the binding reaction can be evaluated according to the Van't Hoff equation:

$$\ln K_b = \frac{\Delta H}{RT} + \frac{\Delta S}{R} \quad (2)$$

where K_b is the binding constant at the corresponding temperature and R is the gas constant. The temperatures used in our experiment were 295, 318 and 338 K, respectively. As we can seen from Fig. 7, the Van't Hoff plot of $\ln K_b$ versus $1/T$ exhibits a very good linearity, allowing us to calculate the enthalpy change (ΔH) and entropy change (ΔS).

Subsequently, the Gibbs free energy change (ΔG) can be estimated from the following equation:

$$\Delta G = \Delta H - T\Delta S \quad (3)$$

The calculated values for ΔH, ΔS and ΔG are listed in Table 1. The positive entropy (ΔS) and negative enthalpy (ΔH) values for the interaction of BSA and GNPs at pH 6 indicate that the electrostatic interactions played a major role in the binding reaction [32], while the negative value of ΔG shows that the binding process is spontaneous. Contrary, at low pH the acting force between BSA and GNPs surface was mainly hydrophobic interaction force.

Table 1
Stern–Volmer quenching constant (K_{SV}) and thermodynamic parameters for BSA binding to GNPs.

pH	Temperature (K)	K_{SV} (mol^{-1} L)	SD[a]	R^b	ΔH (kJ/mol)	ΔS (J/mol K)	ΔG (kJ/mol)
6	295	1.70×10^9	0.0651	0.9994	−28.96	81.35	−48.29
	318	1.41×10^9	0.0782	0.9988			−54.70
	338	9.60×10^8	0.0683	0.9980			−64.32
2	295	1.11×10^9	0.0601	0.9983	10.79	132.87	51.11
	318	6.88×10^8	0.0721	0.9982			53.59
	338	5.05×10^8	0.0700	0.9975			55.22

[a] SD is the standard deviation of the K_{SV} values.
[b] R is the correlation coefficient.

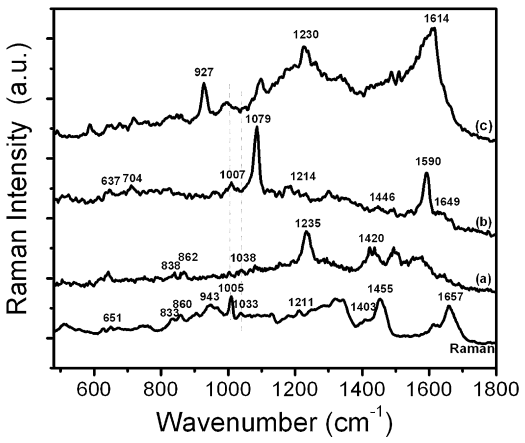

Fig. 8. Raman spectrum of solid BSA and SERS spectra of bioconjugates BSA–GNPs at pH 2 (spectrum c), at pH 6 (spectrum b) and pH 9 (spectrum a).

3.4. SERS investigation of molecular interaction in BSA–GNPs bioconjugates

Specific molecular information concerning the BSA–GNPs interface can be provided by SERS spectroscopy, an ultra-sensitive spectroscopic tool for interface studies. It is well known that the Raman signal of a molecule can be highly amplified by adsorbing the analyte on the surface of GNPs, leading to amplifications up to10^7, by combining the electromagnetic enhancement and chemical charge transfer mechanisms [33]. Fig. 8 depicts the pH-dependent SERS spectra of BSA molecules at pH 9 (spectrum a), at pH 6 (spectrum b) and at pH 2 (spectrum c), together with the normal Raman spectrum of solid BSA (spectrum d), assessing that pH induces great difference at interface. The band assignments for the normal Raman spectrum of BSA and recorded SERS spectra are listed in Table 2. The recorded SERS spectra confirm the change in the α-helix and β-sheet content of the conjugated BSA at different pH values. At neutral pH, BSA protein reveals a heart-shaped molecule and is know to be rich in α-helix structure (about 68%), confirmed in our SERS measurement by an intense band at 1657 cm^{-1} due to the amide I mode as shown in Fig. 8. As such, at neutral pH, the first indication of changes in the secondary structure of BSA due to the protein adsorption onto the GNP surface is suggested by the shift of the amide I band, which is characteristic to the α-helix content in albumin, from 1657 to 1649 cm^{-1} [34]. These spectral changes point out that some of the α-helix structure of BSA may become modified to a β-sheet or random coil conformation due to the interaction with GNP surface. In addition, this observation is sustained by the decrease in the SERS spectrum of the intensity of the skeletal C–C vibration of α-helix conformation at 943 cm^{-1}, indicating its unfolding. The conformational changes of BSA as a function of temperature were investigated by Das et al. by Raman spectroscopy, demonstrating that the secondary structure of albumin is also extremely sensitive to temperature [35]. The contribution from different amino acids can be observed at 1007 and 1033 cm^{-1} (Phe ring breathing), at 1590 cm^{-1} (Trp) and 862, 838 and 1214 cm^{-1} (Tyr). In addition, spectral changes in SERS in the 704–620 cm^{-1} region are due to the νC–S stretching modes of cysteine, the most abundant amino acids in albumin protein, located at position 34 in domain I. However, at low pH values, the amide III band at 1230 cm^{-1} increased in intensity, suggesting a higher contribution from the β-sheet to the albumin structure (see Fig. 8, spectrum c). This means that prior to the molecular expansion of BSA at pH 2, some local disruption of helices can occur. At pH 9, the band at 1420 cm^{-1} due to the symmetric vibration of the COO^- group is significantly enhanced in the SERS spectrum of BSA, suggesting that the carboxyl groups are also interactive with GNPs (see Fig. 8, spectrum a).

Table 2
Band assignments for the normal Raman and SERS spectra of BSA.

BSA (Raman)	BSA pH 2 (SERS)	BSA pH 6 (SERS)	BSA pH 9 (SERS)	Band assignments[a]
1655	1614	1649		Amide I
1580		1590		Phe
1455		1446		δCH_2
1403			1420	COO^-
1211		1214		Phe or Tyr
1033			1038	Phe
1005			1002	Phe
943	927			
860			862	Tyr
833			838	Tyr

[a] Ref. [31].

4. Conclusions

In summary, in this work we have studied the conformational changes induced by pH and temperature on BSA, before and after conjugation with GNPs, using a combination of spectroscopic techniques from LSPR to fluorescence and SERS. The results show that BSA protein in the bioconjugates underwent important conformational changes on both secondary and tertiary structure levels. The thermal denaturation of BSA adsorbed onto the GNPs surface exhibits a distinct behavior compared to BSA in solution, suggesting the possibility of employing GNPs as probes to monitor the thermal denaturation of proteins. Moreover, we use SERS spectroscopy of some specific vibrational bands to follow conformational changes of BSA at metal interface at different pH. These results confirmed that extern stimuli, in this case pH and temperature, greatly influence the nano–bio interfaces, and subsequently the behavior of bioconjugates in biological environments.

Acknowledgment

This work was supported by CNCSIS – UEFISCSU, project number PNII ID_PCCE_129/2008.

References

[1] F. De Angelis, G. Das, P. Candeloro, M. Patrini, M. Galli, A. Bek, M. Lazzarino, I. Maksymov, C. Liberale, L.C. Andreani, E. Di Fabrizio, Nanoscale chemical mapping using three-dimensional adiabatic compression of surface plasmon polaritons, Nat. Nanotechnol. 5 (2010) 67–72.
[2] S. Boca, S. Astilean, Detoxification of gold nanorods by conjugation with thiolated poly(ethylene glycol) and their assessment as SERS-active carriers of Raman tags, Nanotechnology 21 (2010) 235601.
[3] K. Aslan, S.N. Malyn, C.D. Geddes, Metal-enhanced fluorescence from gold surfaces: angular dependent emission, J. Fluoresc. 17 (2007) 7–13.
[4] M. Iosin, P. Baldeck, S. Astilean, Plasmon-enhanced fluorescence of dye molecules, Nucl. Instrum. Meth. B 267 (2009) 403–405.
[5] W. Wang, H. Cui, Chitosan–luminol reduced gold nanoflowers: from one-pot synthesis to morphology-dependent SPR and chemiluminescence sensing, J. Phys. Chem. C 112 (2008) 10759–10766.
[6] B. Kand, M.A. Mackey, M.A. El-Sayed, Nuclear targeting of gold nanoparticles in cancer cells induces DNA damage, causing cytokinesis arrest and apoptosis, J. Am. Chem. Soc. 132 (2010) 1517–1519.
[7] M. Everts, V. Saini, J.L. Leddon, R.J. Kok, M. Stoff-Khalili, M.A. Preuss, C.L. Millican, G. Perkins, J.M. Brown, H. Bagaria, D.E. Nikles, D.T. Johnson, V.P. Zharov, D.T. Curiel, Covalently linked Au nanoparticles to a viral vector: potential for combined photothermal and gene cancer therapy, Nano Lett. 6 (2006) 587–591.
[8] Y. Ding, Z. Chen, J. Xie, R. Guo, Comparative studies on adsorption behavior of thionine on gold nanoparticles with different sizes, J. Colloid Interf. Sci. 327 (2008) 243–250.
[9] P. Roach, D. Farrar, C.C. Perry, Interpretation of protein adsorption: surface-induced conformational changes, J. Am. Chem. Soc. 127 (2005) 8168–8173.

[10] S.H. Brewer, W.R. Glomm, M.C. Johnson, M.K. Knag, S. Franzen, Probing BSA binding to citrate-coated gold nanoparticles and surfaces, Langmuir 21 (2005) 9303–9307.
[11] S.H. De Paoli Lacerda, J.J. Park, M. Meuse, D. Pristinski, M.L. Becker, A. Karim, J.F. Douglas, Interaction of gold nanoparticles with common human blood proteins, ACS Nano 4 (2010) 365–379.
[12] Y. Guo, Y. Ma, L. Xu, W. Yang, Conformational change induced reversible assembly/disassembly of Poly-L-lysine functionalized gold nanoparticles, J. Phys. Chem. C 111 (2007) 9126–9127.
[13] M. Iosin, F. Toderas, P. Baldeck, S. Astilean, Study of protein-gold nanoparticle conjugates by fluorescence and surface-enhanced Raman scattering, J. Mol. Struct. 924–926 (2009) 196–200.
[14] I. Dalle-Donne, A. Scaloni, D. Giustarini, E. Cavarra, G. Tell, G. Lungarella, R. Colombo, R. Rossi, A. Milzani, Proteins as biomarkers of oxidative/nitrosative stress in diseases: the contribution of redox proteomics, Mass Spectrom. Rev. 24 (2005) 55–99.
[15] S.J. McClellan, E.I. Franses, Effect of concentration and denaturation on adsorption and surface tension of bovine serum albumin, Colloids Surf. B: Biointerfaces 28 (2003) 63–75.
[16] A.G. Tkachenko, H. Xie, D. Coleman, W. Glomm, J. Ryan, M.F. Anderson, S. Franzen, D.L. Feldheim, Multifunctional gold nanoparticle peptide complexes for nuclear targeting, J. Am. Chem. Soc. 125 (2003) 4700–4701.
[17] T. Peters Jr., All About Albumin, Academic Press, New York, 1996.
[18] J. Turkevich, P.C. Stevenson, J. Hillier, A study of the nucleation and growth processes in the synthesis of colloidal gold, Discuss. Faraday Soc. 11 (1951) 55–75.
[19] R.E. Georgescu, E.G. Alexov, M.R. Gunner, Combining conformational flexibility and continuum electrostatics for calculating pK_as in proteins, Biophys. J. 83 (2002) 1731–1748.
[20] P.A. Zunszain, J. Ghuman, T. Komatsu, E. Tsuchida, S. Curry, Crystal structural analysis of human serum albumin complexed with hemin and fatty acid, BMC Struct. Biol. 3 (2003) 1–9.
[21] I. Lynch, T. Cedervall, M. Lundqvist, C. Cabaleiro-Lago, S. Linse, K.A. Dawson, The nanoparticle–protein complex as a biological entity; a complex fluids and surface science challenge for the 21st century, Adv. Colloid Interf. Sci. 134–135 (2007) 167–174.
[22] L. Shang, Y. Wang, J. Jiang, S. Dong, pH-dependent protein conformational changes in albumin:gold nanoparticle bioconjugates: a spectroscopic study, Langmuir 23 (2007) 2714–2721.
[23] P.L Gentili, F. Ortica, G. Favaro, Static and dynamic interaction of a naturally occurring photochromic molecule with bovine serum albumin studied by UV–visible absorption and fluorescence spectroscopy, J. Phys. Chem. B 112 (2008) 16793–16801.
[24] Y.Q. Wang, H.M. Zhang, G.C. Zhang, Q.H. Zhou, Z.H. Fei, Z.T. Liu, Z.X. Li, Fluorescence spectroscopic investigation of the interaction between benzidine and bovine hemoglobin, J. Mol. Struct. 886 (2008) 77–84.
[25] M.R. Eftink, C.A. Ghiron, Exposure of tryptophyl residues inproteins. Quantitative determination by fluorescence quenching studies, Biochemistry 15 (1976) 672–679.
[26] J.R. Lakowicz, Principles of Fluorescence Spectroscopy, 3rd ed., Plenum Press, New York, 2006.
[27] T. Hiratsuka, Conformational changes in the 23-Kilodalton NH_2-terminal peptide segment of myosin ATPase associated with ATP hydrolysis, J. Biol. Chem. 265 (1990) 18786–18790.
[28] M.R. Eftink, The use of fluorescence methods to monitor unfolding transitions in proteins, Biochemistry (Moscow) 63 (1998) 276–284.
[29] M. Rezaei-Tavirani, S.H. Moghaddamnia, B. Ranjbar, M. Amani, S.A. Marashi, Conformational study of human serum albumin in pre-denaturation temperatures by differential scanning calorimetry, circular dichroism and UV spectroscopy, J. Biochem. Mol. Biol. 39 (2006) 530–536.
[30] V.J.C. Lin, J.L. Koenig, Raman studies of bovine serum albumin, Biopolymers 15 (1976) 203–218.
[31] L.Z. Zhao, R.T. Liu, X.C. Zhao, B.J. Yang, C.Z. Gao, X.P. Hao, Y.Z. Wu, New strategy for the evaluation of CdTe quantum dot toxicity targeted to bovine serum albumin, Sci. Total Environ. 407 (2009) 5019–5023.
[32] D.P. Ross, S. Subramanian, Thermodynamics of protein association reactions: forces contributing to stability, Biochemistry 20 (1981) 3096–3102.
[33] M. Baia, F. Toderas, L. Baia, J. Popp, S. Astilean, Probing the enhancement mechanisms of SERS with p-aminothiophenol molecules adsorbed on self-assembled gold colloidal nanoparticles, Chem. Phys. Lett. 422 (2006) 127–132.
[34] X.C. Shen, X.Y. Liou, L.P. Ye, H. Liang, Z.Y. Wang, Spectroscopic studies on the interaction between human hemoglobin and CdS quantum dots, J. Colloid Interf. Sci. 311 (2007) 400–406.
[35] G. Das, F. Mecarini, F. Gentile, F. De Angelis, H.G. Mohan Kumar, P. Candeloro, C. Liberale, G. Cuda, E. Di Fabrizio, Nano-patterned SERS substrate: application for protein analysis vs. temperature, Biosens. Bioelectron. 24 (2009) 1693–1699.